

Visualisation and characterisation of electrical contact spots for different current values using X-ray computer tomography

C. Roussos & J. Swingler

*School of Engineering and Physical Sciences,
Heriot-Watt University, UK*

Abstract

Electrical contact is an important parameter for the reliability of electrical devices. Due to the limitation of optical imaging, methods available for the contact measurement characteristics are only suitable for open or transparent systems. For most of the practical situations that require contact measurement characteristics in non-transparent or enclosed systems, the traditional methods are not effective. Based upon these requirements, a method suitable for the electrical contact characteristics in non-transparent systems is developed by using X-ray computer tomography (CT). The main advantage of this visualisation method is the ability to acquire three-dimensional (3D) views of systems keeping the features intact. In this work, the method is demonstrated by measuring the contact area and the average contact angle in each contact spot which is held between the conductors of 16A AC single pole switch after two different current tests (0 and 16A AC). The distances between the contact spots are also calculated.

Keywords: X-ray CT, contact angle distribution, contact area distribution, distance distribution.

1 Introduction

Real surfaces show on the microscopic scale peaks and valleys which present a roughness with fractal behaviour are found to be very interesting by a lot of research [1–5]. When the roughness of two surfaces are brought together they influence mechanical contact which occur only in a specific number of areas on the apparent area of contact.



Bhushan [6], demonstrated the contact interface by using the fractal behaviour of natural phenomena of a surface. This approach illustrates that the asperity curvature and slope depend on the measurement resolution and the statistical sample size. For example, for a coarse measurement of resolution, only a few asperities of large curvature are observed while for smaller measurement of resolution more asperities of smaller curvature are observed [7]. Scale dependency can be eliminated if the fractal approach is applied which is a possible technique to characterise the surface using parameters such as the scaling parameter and fractal dimension. An understanding of contact phenomena that occurs at a contact interface is crucial to achieve better performance and long-term reliability of devices consisting such interfaces.

There are many techniques that can be used to visualise the contact area. These techniques can be categorized into destructive and non-destructive. Destructive techniques involving scanning electron microscopy [8] and thermo-graphic [9] can be applied if one part of the interface is substituted to enable the viewing of the interface, or if both parts of the original contact are investigated, they need to be dismantled after testing for analysis. Non-destructive techniques involving magnetic resonance imaging (MRI) [10] and X-ray CT [11–14] are of more interest because they offer the possibility to acquire 2D and 3D views of samples without dismantling the component parts and thus destroy any features of interest.

Most previous contact area visualisation techniques do not consider the effects of scale dependent properties; in fact, many classical and widely used contact area visualisation techniques completely neglect the effect of scaled contact areas. The aim of the current work is to build on the visualisation technique developed in previous work [14] which the actual contact interface is pictured in a 3D plane as a “3D Contact Map”.

The mechanical area of contact can be calculated using different methods [15–17]. One of these methods belongs to Bowden and Tabor [15] who showed that the total mechanical area A , of contact under plastic deformation of the asperities flowing when loaded with force, F is given by eqn (1). Where H , is the hardness of the material. This method proved by Lalechos *et al.* [13] is very useful for the electrical contact theory as it gives values close to experimental findings.

$$A = \frac{F}{H} \quad (1)$$

Bhushan [6], picks out and emphasizes the importance of area and spatial distributions of contact spots in elaborating theories in contact physics and tribology. The contact spot spatial distribution is significant in working at the stress and dynamic interactions between contact spots. In an electrical contact, the contact spot area and spatial distributions are significant as they have been used by many researchers [16, 18, 19] to develop expressions to model the contact resistance.

Swingler and Lalechos in [20] and Swingler in [21] show that the area cumulative distribution of the contact spots in 2D plane followed a Korcak-type distribution similar to the spatial cumulative distribution neglecting the effects of differences in scale. The contact spot area cumulative distribution shows the

number of contact spots with the area equal or greater than a reference area, A_{ref} as described in eqn (2). Where A_L , is the area of the largest contact spot and D is the size fractal dimension.

$$N(A_i \geq A_{ref}) = \left(\frac{A_L}{A_{ref}} \right)^{\frac{D}{2}} \quad (2)$$

The cumulative spatial distribution shows the number of contact spots with the separation S_{ij} equal or greater than a reference contact spot separation S_{ref} as described in eqn (3). Where n_{res} , is the number of contact spots i , separated from contact spots j by the resolution of the technique, S_{res} (pixel length). Where D_s , is the contact spot separation fractal dimension.

$$N_s(S_{ij} \leq S_{ref}) = n_{res} \left(\frac{S_{ref}}{S_{res}} \right)^{D_s} \quad (3)$$

Jang and Jang [22] reported that the scale dependency of contact distributions should be considered; because contact spots are formulated by rough surfaces at different scales having different morphologies. They worked on area and spatial distributions of contacts in random fractal surfaces and natural contacts (real islands). The distribution of the contact spots is investigated when the surface is cut at any given height. Jang and Jang [22] used the same procedure as Swingler in [21] to investigate the multi-scale area and spatial distributions of contact spots. Using this procedure, they analysed the area and spatial distribution of natural contact spots for different scales and demonstrated that the area and spatial distribution of random and natural contact spots are following the Korcak-type empirical relationship.

The work presented in this paper focuses on the calculation of contact spots characteristics in 3D contact maps where the scale dependency of contact spot distributions is considered. The calculations include the contact spot areas, angles and spatial distributions of 16A AC single pole switch after two current tests at 0A and 16A AC.

2 Experimental method

2.1 Sample

The sample is a contact arrangement from a single pole rocker switch rated at 16A AC. The contact material is made of a silver alloy while other conductors are made from a copper alloy. The internal view of the metalwork of the switch is illustrated in fig. 1a). It consists of conductors, contact pair and a contact force spring. The close-up view of a closed contact pair of the single pole switch which is the volume of interest is illustrated in fig. 1b). For the 3D visualization of the close-up view of a closed contact pair, “CATVIn” analysis tool and “ImageVis3D” software are used as described in [14].

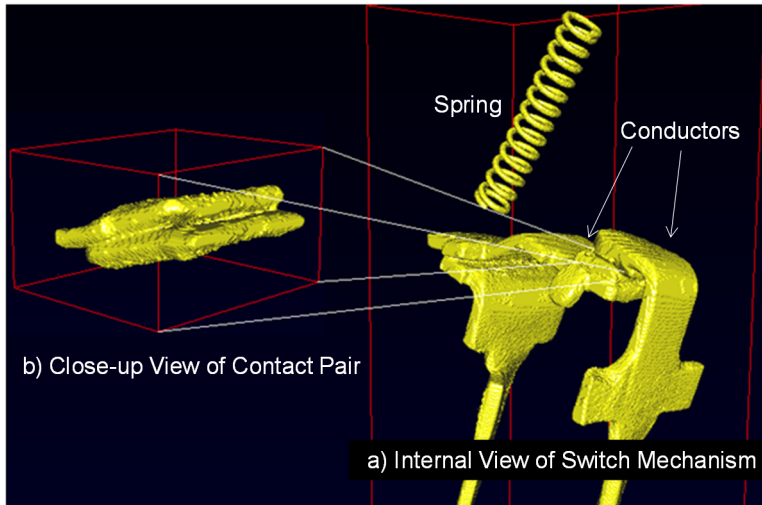


Figure 1: Internal view of switch mechanism.

2.2 Data acquisition

The visualisation of the contact interface as a 3D contact map has been previously presented in more detail in [14] as the “CATCM”. This paper discusses the X-ray CT scanning procedure and highlights in detail the analysis techniques which are used for the development and visualisation of the contact interface as a 3D contact map.

For the data acquisition an HMX 225 μ CT system is used. The system operates using X-ray tomography processing designed in collaboration with XTek Group. The X-ray source is set to 175kV, 133 μ A, which gives 5.2 μ m focus capability.

The scanner rotates a sample through 360°, taking a series of 2D X-ray images (2439 images are taken). In the process the 2D X-ray images are reconstructed as a 3D model using the “CT-Pro” software. The software “VGStudioMax” is then used to create 2D cross-sectional slice images (791 images are taken) from the 3D model.

Fig. 2 shows an example of a 2D cross-sectional slice image where the conductors of 16A AC single pole switch can be clearly seen. The resolution of these images using a suite of Contact Analysis Techniques (CAT*) [14] to render the 3D is contact map which identifies the contact areas between the two conductors.

3 Results and analysis

3.1 3D contact maps

Fig. 3 shows two different 3D contact maps of the contacting interface of the single pole switch contacts with pixel length equal with $4.95 \pm 0.05\mu$ m. These maps are

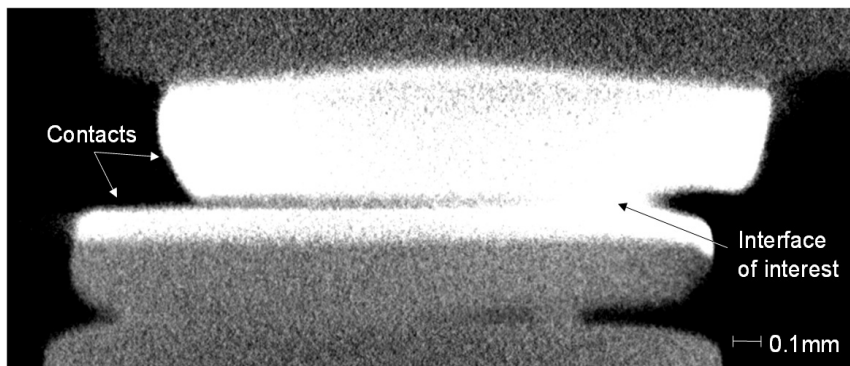


Figure 2: 2D cross-sectional slice image.

for the same switch which is scanned twice. The first scan (for the 3D contact map, fig. 3a)) is after non-current loading and the second (for the 3D contact map, fig. 3b)) is after current loading at 16A AC for 48 hours and stored in the lab for ~30 days.

3.2 Contact spot area distribution

Fig. 4 is a set of graphs showing the contact spot area distribution for different current values. The data are taken from the 3D contact maps represented in fig. 3. The area of each contact spot is defined as the sum of pixels within the contact spot. The smallest area of contact spot indicated on the graphs is 1 pixel, which is the resolution of the technique ($1 \text{ pixel} = 25 \mu\text{m}^2$), and the largest spots indicated are several hundred pixels in area. The number of contact spots at 0A is counted to 610 and at 16A is reduced to 247.

3.3 Contact spot nearest neighbour spatial distribution

Fig. 5 is a set of graphs showing the contact spot nearest neighbour spatial distribution for different current values from the data taken from 3D contact maps represented in fig. 3. The spatial difference between contact spots can be defined by several methods. In this work, the spatial difference between contact spots is defined as the distance between the centroid of each contact spot from the others. The nearest neighbour distribution is plotted in fig. 5. The smallest distance between two contact spots indicated on the graphs is $\sqrt{2}$ pixel length and the bigger distances are several dozen pixel length. The distance values presented in fig. 5 are rounded towards the integer, resulting in an array of integers.

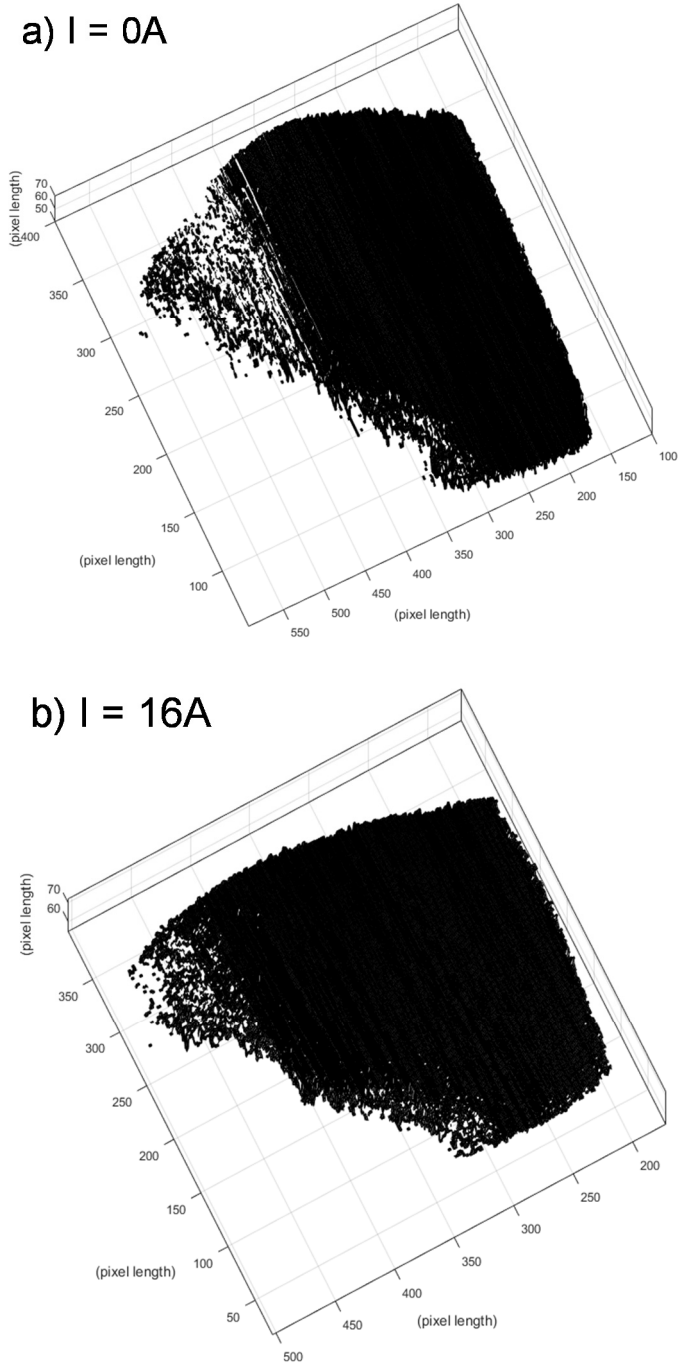


Figure 3: 3D contact maps.

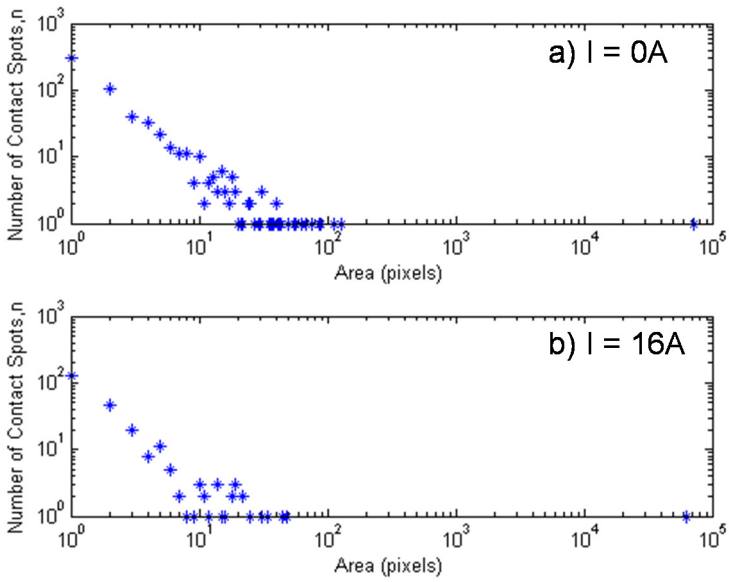


Figure 4: Contact spot area distribution.

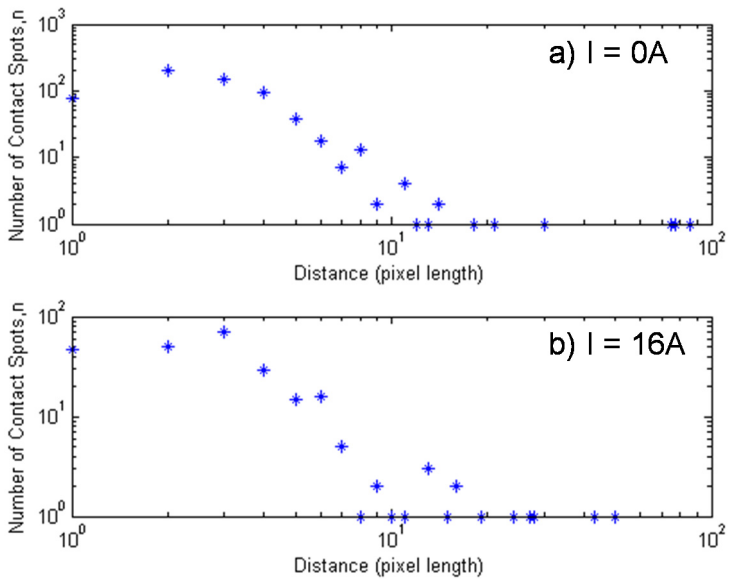


Figure 5: Contact spot nearest neighbour spatial distribution.

3.4 Contact spot angle distribution

Fig. 6a) and 6b) are a set of graphs showing the contact spot angle distribution for different current values from the data taken from 3D contact maps represented in fig. 3. The angle of each contact spot in this work is defined as the average angle calculated from the slope of neighbour pixels within the contact spots. All the angle values presented in fig. 6 are rounded towards the integer, resulting in an array of integers. Fig. 6c) illustrates the contact spot angle distributions of fig. 6a) and 6b) on the same graph which their points are connected with lines. The contact spot angle distribution takes values from $\sim -80^\circ$ to $\sim 80^\circ$.

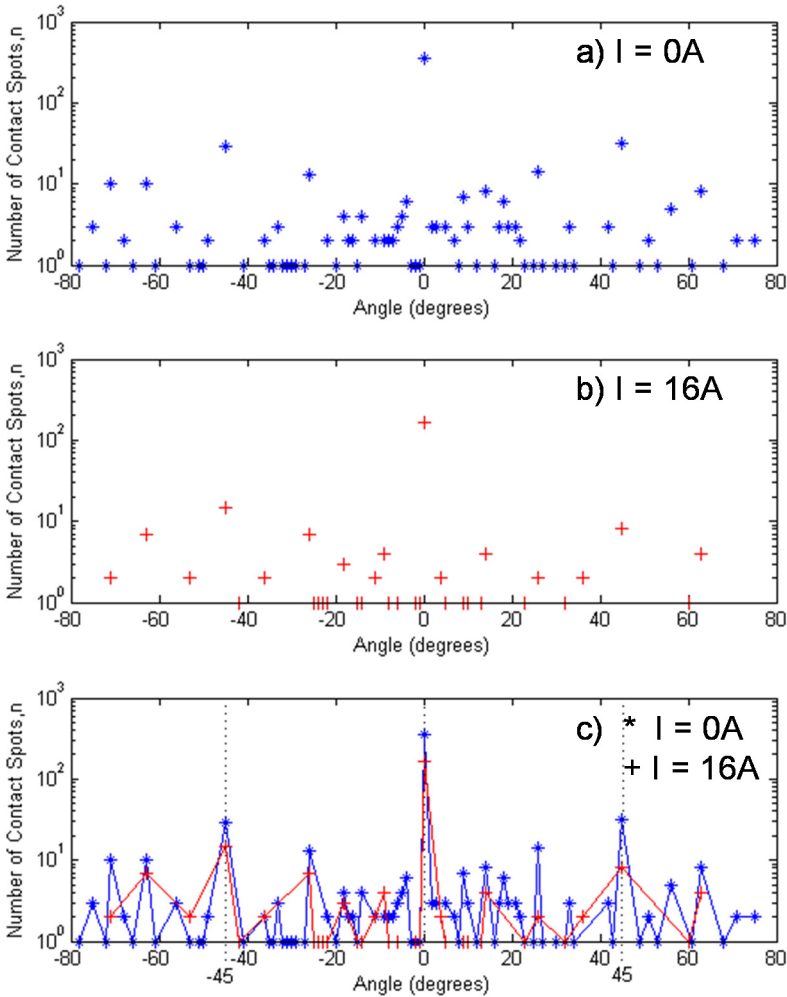


Figure 6: Contact spot angle distribution.

4 Discussion

The results show that the X-ray CT is a powerful method for viewing and characterising the contact interface without dismantling the sample keeping the features intact. The 2D cross-sectional images obtained in this work with the current facility give a resolution of $4.95 \pm 0.05 \mu\text{m}$ which is 5.5 times more pure than previous work [11].

The X-ray CT method is found suitable for the consideration of scale dependency of contact spots which are presented in 3D contact maps using a suite of CAT* [14]. The scale dependency is important for the consideration of contact spots as mentioned by Jang and Jang [22] because they are formulated by rough surfaces at different scales resulting in different morphologies.

The graphs of contact spot area distribution in fig. 4 show that the contact spots follow the same distribution under different current values. These graphs can be compared with the corresponding graphs in Swingler and Lalechos work [20] which visualises the contact area in 2D contact maps under different contact forces. The results show that the area of contact spots follow the same distribution in both situations. The total contact area at 0A is equal with 75,977 pixels having 610 contact spots with the largest contact spot equal with 72,760 pixels. At 16A the total contact area is reduced to 63,612 pixels having 247 contact spots with the largest contact spot equal with 62,726 pixels.

The graphs of contact spot nearest neighbour spatial distribution in fig. 5 show that the contact spots follow similar distribution under different current values. The biggest distance between two contact spots at 0A is calculated equal with 86 pixel length and at 16A is calculated equal with 50 pixel length. Moreover, the majority of contact spots at 0A have distance 2 pixel length while at 16A distance is increasing to 3 pixel length. Furthermore, it could be interesting to calculate the minimum distance distributions between the contact spots and compare the results with the presented results.

The results of contact spot area and contact spot spatial distributions can be used for the calculation of contact spot area and spatial cumulative distributions in order to identify the fractal characteristics of electrical contact spots under different current values. These results can be also compared with Swingler [21] and Jang and Jang works [22].

The graphs of contact spot angle distribution in fig. 6a and 6b show that the contact spots follow same the distribution under different current values. This distribution is presented in fig.6c whose points are connected with lines and present peaks and valleys like spectral density plot with angular spatial frequency [6]. The distribution in negative axis can be characterised as a reflection in positive axis and vice versa. Moreover, the graphs in fig. 6 show that the maximum number of contact spots have an angle equal with 0° and the angles with values equal with -45° and 45° follow in number of contact spots.

The results of contact spot angle distribution are found to be very interesting as they present angles with “reflection” between the positive and negative axes. This phenomenon should be examined if still appeared for different current values and different contact arrangements. Moreover, it could be examined if there is any

relation between the locations of contact spots in the 3D contact map with their angles.

5 Conclusion

The X-ray CT method has been used to produce 3D visualisation of a contact arrangement from a single pole rocker switch rated at 16A AC without the need to dismantle the sample. The real contact interface using this method is visualised after two different current tests (0A and 16A).

The contact area and average contact angle of each contact spot are calculated and presented with their distributions after the two current test. The distances between the centroids of contact spots are also calculated and presented with their distributions. For all the calculations, the scale dependency is considered because contact spots are formulated by rough surfaces at different scales having different morphologies.

Analytical tools are under development to calculate the minimum distance distribution of contact spots and their cumulative area and spatial distributions in order to identify their fractal characteristics in 3D interfaces.

Acknowledgements

This work is supported by DTA studentship funded by EPSRC. Additionally, it is supported by the National Institute of General Medical Sciences of the National Institutes of Health under grant number P41GM103545 and the DOE SciDAC Visualization and Analytics Center for Enabling Technologies, DEFC0206ER25781.

References

- [1] Kogut, L. & Komvopoulos, K., Electrical contact resistance theory for conductive rough surfaces. *Journal of Applied Physics*, **94(5)**, pp. 3153-3162, 2003.
- [2] Majumdar, A. & Bhushan, B., Fractal Model of Elastic-Plastic Contact between Rough Surfaces. *Journal of Tribology* **113(1)**, pp. 11-22, 1991.
- [3] Palasantzas, G. & Hosson, J. T. M. D., Self-affine roughness effects on the contact area between elastic bodies. *Journal of Applied Physics*, **93(2)**, pp. 898-902, 2003.
- [4] Borodich, F. M. & Mosolov, A. B., Fractal roughness in contact problems *Journal of Applied Mathematics and Mechanics*, **56(5)**, pp. 681-690, 1992.
- [5] Borodich, F. M. & Onishchenko, D. A., Similarity and fractality in the modelling of roughness by a multilevel profile with hierarchical structure. *International Journal of Solids and Structures*, **36(17)**, pp. 2585-2612, 1999.
- [6] Bhushan, B., *Handbook of Micro/Nanotribology*, CRC Press: Boca Raton, FL, 1999.



- [7] Ciavarella, M., Demelio, G., Barber, J. R. & Jang, Y. H., Linear elastic contact of the Weierstrass profile. *Proceedings of the Royal Society of London. Series A*, **456**, pp. 387-405, 2000.
- [8] Goldstein, J., Newbury, D. E., Joy, D. C., Lyman, C. E., Echlin, P., Lifshin, E., Sawyer, L. & Michael, J. R., *Scanning Electron Microscopy and X-Ray Microanalysis*, Springer: New York, 2003.
- [9] Myers, M., Leidner, M. & Schmidt, H., Effect of Contact Parameters on Current Density Distribution in a Contact Interface. *Proc. of the 57th IEEE Holm Conference on Electrical Contacts*, IEEE: Minneapolis, MN, pp. 1-9, 2011.
- [10] Zhu, W., Tian, Y., Gao, X. & Jiang, L., A Method To Measure Internal Contact Angle in Opaque Systems by Magnetic Resonance Imaging. *Langmuir: The ACS journal of surfaces and colloids*, **29**, pp. 9057-9062, 2013.
- [11] Roussos, C. & Swingler, J., Evaluation of Electrical Contacts Using an X-Ray CT 3D Visualisation Technique. *Proc. of the 27th International Conference on Electrical Contacts (ICEC 2014)*, VDE: Dresden, Germany, pp. 326-331, 2014.
- [12] Lalechos, A. V., Swingler, J. & Crane, J., Visualisation of the Contact Area for Different Contact Forces using X-Ray Computer Tomography *Proc. of the 54th IEEE Holm Conference on Electrical Contacts*, IEEE: Orlando, FL, pp. 263-269, 2008.
- [13] Lalechos, A. V., Swingler, J. & McBride, J. W., Evaluation of the X-Ray CT Visualisation Technique for Characterising Electrical Contacts. *Proc. of the 56th IEEE Holm Conference on Electrical Contacts*, IEEE: Charleston, SC, pp. 1-6, 2010.
- [14] Roussos, C. & Swingler, J., Contact analysis and modeling of 3D visualization data of real un-dismantled electrical contact interfaces. *Submitted to Wear*, 2014.
- [15] Bowden, F. P. & Tabor, D., Area of Contact between Solids. *The friction and lubrication of solids*, Clarendon Press: Oxford, 2001.
- [16] Holm, R., Theory and Applications *Electric Contacts*, Springer: Berlin, 1967.
- [17] Mindlin, R. D., Compliance of Elastic Bodies in Contact. *Journal of Applied Mechanics*, **16**, pp. 259-268, 1949.
- [18] Greenwood, J. A., Constriction resistance and the real area of contact. *Journal of Applied Physics*, **17**, pp. 1621-1632, 1966.
- [19] Holm, R., *Electric Contacts Handbook* Springer Verlag: Berlin, 1958.
- [20] Swingler, J. & Lalechos, A., Visualization and size distribution of contact spots at a real un-dismantled electrical contact interface. *Journal of Physics D: Applied Physics*, **42(8)**, pp. 1-7, 2009.
- [21] Swingler, J., The resolution dependence of measured fractal characteristics for a real un-dismantled electrical contact interface. *Wear*, **268(9-10)**, pp. 1178-1183, 2010.
- [22] Jang, J. & Jang, Y. H., Spatial distributions of islands in fractal surfaces and natural surfaces. *Chaos, Solitons & Fractals*, **45(12)**, pp. 1453-1459, 2012.